DOI: 10.1002/cphc.201100650

Conformational Flexibility of Glycosylated Peptides

Stefan Bollmann,[a] Anne Burgert,[a] Carolin Plattner,[b] Lilly Nagel,[b] Norbert Sewald,[b] Marc Löllmann,[a] Markus Sauer,[a] and Sören Doose*[a]

Glycosylation adds carbohydrate moieties to proteins and functional peptides. Glycans, highly branched carbohydrate heteropolymers that can be attached to amino acids either through *N*- or *O*-glycosylation, serve as coding entity, providing specificity for carbohydrate–protein interactions, or modifying dynamic and structural behaviour of proteins. Glycoconjugates present glycans of extraordinary large structural variety, enabling information coding by steering molecular recognition.[1] Glycosylated proteins and lipids usually present their glycan moieties solvent-exposed at the surface where they can serve as highly specific binding partners. Specific protein–glycan interactions generally are enthalpically driven through hydrogen bonding and van der Waals interactions. Strong interactions only come about through cooperative formation of many hydrogen bonds or hydrophobic interactions. Glycoproteins and -lipids contribute to a range of signaling interactions mostly in eukaryotic cells, help regulate cell–cell communication and immune response,[2] or control protein folding and turnover.[3] Often a protein's functional state or specific complex is stabilized by glycosylation analogous to the effects of molecular crowding.[3b,c] Glycoproteins also serve as antifreeze reagent when interacting with ice crystals.[4]

Since glycoproteins often are partially or fully disordered and glycans themselves are highly flexible structures,[5] the question arises how conjugated glycans influence protein and peptide conformational dynamics. Extensive *O*-glycosylation of mucin-like glycopeptides seems to rigidify the peptide backbone and increase the overall radius of gyration.[6] The unfolded state in a dynamic folding/unfolding protein equilibrium is influenced by glycosylation, too.[3b] However, various and partly contradictory effects of *N*/*O*-glycosylation on peptide conformations were observed experimentally and in computer simulations.[5,7] Overall, there is no comprehensive understanding on the molecular scale how glycoconjugate conformational dynamics are shaped by glycans and we seek to address this issue by studying well-defined synthetic model peptides.

Herein we give an account of the influence that β-galactose *O*-conjugated to serine residues impose on peptide conformational dynamics. We compare intramolecular dynamics of unstructured peptides made of either glycine–serine repeats [Gly-Ser] or made of glycosylated serine–glycine repeats [Ser(β-Gal)-Gly)] and characterize influences from attached glycans on peptide dynamics. Conformational dynamics are monitored and analyzed by fluorescence correlation spectroscopy (FCS).[8] As reporter system for dynamic processes we introduce a fluorophore–quencher pair on opposite ends of the unstructured peptides that report on end-to-end contacts by on/off changes in the fluorescence emission. We use the oxazine fluorophore MR121 (Figure 1), attached via site-specific labeling chemistry to the N-terminus, and the fluorescence-quenching amino acid tryptophan (Trp), incorporated as last residue on the C-terminus. Fluorescence quenching occurs due to photoinduced electron transfer (PET) and was shown to be an ideal reporter system for monitoring conformational dynamics of biopolymers at low (nanomolar) concentrations and on short (nano- to microsecond) time scales.[9] We compared end-to-end contact kinetics side by side as function of temperature and solvent viscosity. The study reveals that *O*-glycosylated β-galactose on each serine residue significantly reduces end-to-end contact rates.

As model compounds we synthesized MR121-[Ser(β-Gal)-Gly-]$_8$Trp peptides in which each serine residue was modified by a single β-galactose unit (Figure 1). Peptides were synthesized by solid-phase synthesis with glycosylated dipeptides as building blocks. Dipeptides were prepared by coupling of Fmoc-Ser-OH to H-Gly-O*t*Bu·HCl using HBTU and HOBt. The reaction resulted in the protected dipeptide Fmoc-Ser-Gly-O*t*Bu. Subsequently the hydroxyl function in the side chain of the serine residue was glycosylated with penta-*O*-acetyl-β-D-galactose in

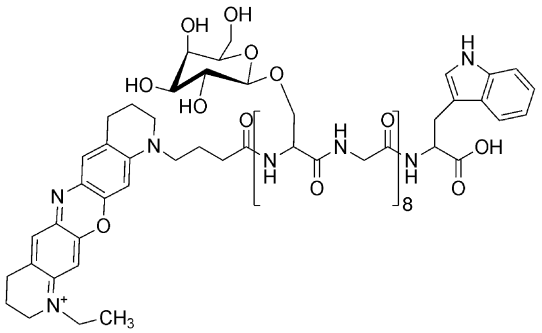

Figure 1. Chemical structure of fluorescence-labeled glycopeptide MR121-[Ser(β-Gal)-Gly-]$_8$Trp. The fluorescent oxazine dye MR121 is quenched upon contact with the tryptophan side chain. Each serine is *O*-glycosylated with β-galactose.

[a] *S. Bollmann, A. Burgert, Dr. M. Löllmann, Prof. Dr. M. Sauer, Dr. habil. S. Doose*
Department of Biotechnology and Biophysics
Julius Maximilians University
97074 Würzburg (Germany)
Fax: (+49) (931) 3184509
E-mail: soeren.doose@uni-wuerzburg.de

[b] *Dr. C. Plattner, L. Nagel, Prof. Dr. N. Sewald*
Department of Chemistry
Bielefeld University
Universitätsstr. 25, 33615 Bielefeld (Germany)

Supporting information for this article is available on the WWW under http://dx.doi.org/10.1002/cphc.201100650.

a $BF_3{\cdot}OEt_2$-mediated reaction, giving exclusively the β-anomer of the glycosylated dipeptide with a free C-terminus. Peptide synthesis was accomplished by fragment condensation on solid phase using Fmoc-Ser(β-Ac_4Gal)-Gly-OH as the building block followed by purification by HPLC (see Supporting Information for details). All peptides were characterized by reverse-phase liquid chromatography and mass spectrometry.

For direct comparison of glycosylated and non-glycosylated peptides, we investigated MR121-[Ser(β-Gal)-Gly-]$_8$Trp and compared the results to previous studies and new control measurements of MR121-[Gly-Ser-]$_8$Trp. We measured an overall steady-state fluorescence quantum yield QY_{ss} [that is the ratio of fluorescence emission from a peptide with (I) and without (I_0) quencher involved] of $QY_{ss}=I/I_0=0.54\pm0.04$ for MR121-[Ser(β-Gal)-Gly-]$_8$Trp (at 20 °C) as compared to $QY_{ss}=0.44\pm0.05$ for MR121-[Gly-Ser-]$_8$Trp (interpolated from two measurements for MR121-[Gly-Ser-]$_7$Trp and MR121-[Gly-Ser-]$_9$Trp). Fluorescence lifetime measurements by time-correlated single-photon counting (TCSPC) were performed to estimate the dynamic quantum yield QY_{dyn}, which reports on collision-induced fluorescence quenching,[10] and the static quantum yield $QY_{st}=QY_{ss}/QY_{dyn}$, which reports on fluorescence quenching due to complex formation. The dynamic quantum yield $QY_{dyn}=\tau/\tau_0=0.96\pm0.02$ for MR121-[Ser(β-Gal)-Gly-]$_8$Trp is much larger than $QY_{st}=0.56\pm0.06$ and similar to those measured for MR121-[Gly-Ser-]$_8$Trp ($QY_{dyn}=0.88\pm0.02$ and $QY_{st}=0.50\pm0.06$), thus confirming that quenching is mostly due to static quenching from formation of stacked complexes as described previously.[9a,b]

Fluorescence fluctuations due to translational diffusion through the confocal observation volume (on millisecond time scales) and due to contact formation and opening processes of the reporter system (on nano- to microsecond time scales) were recorded and analyzed by FCS (Figure 2). FCS data could all be fitted with a simple diffusion model and a single or double exponential decay function for the fast phase of the correlation decay [Eq. (S2), Supporting Information]. A small-amplitude phase on microsecond time scales with an amplitude of <0.05 that results from intersystem crossing of MR121 does not have a significant influence on all other fit parameters.

Focusing on the millisecond phase of the correlation decay we estimated the translational diffusion constant D of MR121-[Gly-Ser-]$_8$Trp and MR121-[Ser(β-Gal)-Gly-]$_8$Trp from FCS measurements in a temperature range from 5 to 40 °C and found significant smaller D values for glycosylated peptides. According to the Stokes–Einstein equation D is related to an average hydrodynamic radius R_h as $D=k_BT/6\pi\eta R_h$ (with Boltzmann constant k_B, temperature T, viscosity η). In Figure 3 diffusion constants for MR121-[Ser(β-Gal)-Gly-]$_8$Trp and MR121-[Gly-Ser-]$_8$Trp are plotted as function of $T/\eta(T)$ and fitted by linear regression confirming the Stokes–Einstein relation. From the fit we estimated the relation of R_h of non-glycosylated to glycosylated peptides $R_h(-\text{Gal})/R_h(+\text{Gal})$ to be 0.74 ± 0.03. The number confirms that the glycopeptide is slightly expanded spending less time in the closed conformation with the reporter system in contact.

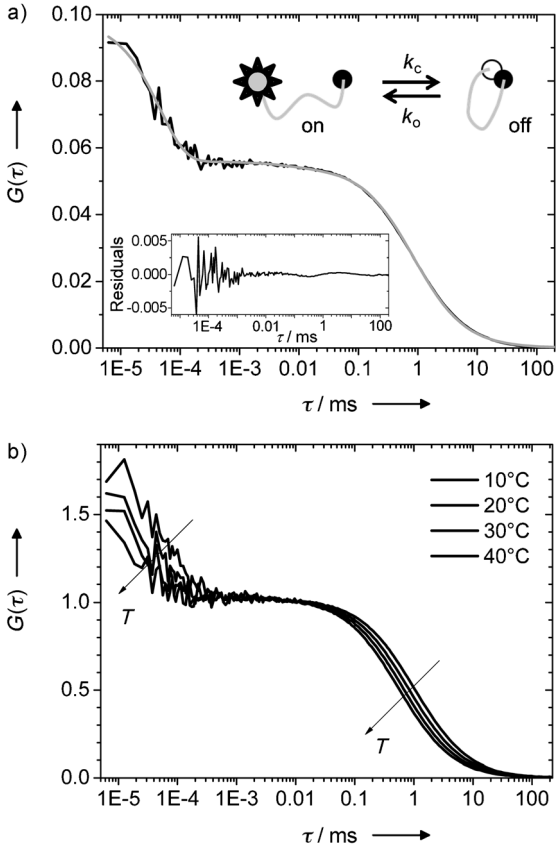

Figure 2. a) FCS data for MR121-[Ser(β-Gal)-Gly-]$_8$Trp measured at 20 °C in aqueous solution. The data fits well to a single-exponential decay on ns times and a diffusion decay on ms times [Eq. (S2), Supporting Information]. Residuals are shown as inset. b) FCS data measured at temperatures of 10, 20, 30, and 40 °C plotted after normalization to the same diffusion-term amplitude.

The amplitude of the fast phase of the correlation decay $K=c_c/c_o$ (with concentration $c_{c/o}$ of peptides in their closed/open state) results from formation of quenched MR121-Trp complexes reporting on the end-to-end contact formation and is a measure of the static quantum yield $QY_{st}=1/(K+1)$. For example, at 20 °C we measure $K=0.61\pm0.01$, which corresponds to an ensemble estimate of $QY_{st}=0.62\pm0.01$. The complex forms due to short-range hydrophobic interactions and is not rate-limiting for end-to-end contact formation rates, as was demonstrated before with unmodified MR121-[Gly-Ser-]$_x$Trp.[9d,11]

In aqueous solution all fast correlation decays are well described by a single exponential decay corresponding to a two-state system (Figure 2). We derived end-to-end contact formation and opening rate constants k_c and k_o from amplitude K and relaxation time t_{rel} according to $K=k_c/k_o$ and $t_{rel}=1/(k_c+k_o)$. Assuming the power law dependence of contact rates as described previously,[9d,11] we estimated contact rate constants for MR121-[Gly-Ser-]$_8$Trp of $k_c=(2.9\pm0.5)\times10^7\ s^{-1}$ at 20 °C (which were confirmed on the current setup). For MR121-[Ser(β-Gal)-Gly-]$_8$Trp we measured a contact rate constant of $k_c=(0.8\pm0.1)\times10^7\ s^{-1}$ which is smaller by a factor between three and four. In order to illuminate how glycans slow down end-to-end contact formation, we performed temperature- and viscosity-dependent measurements.

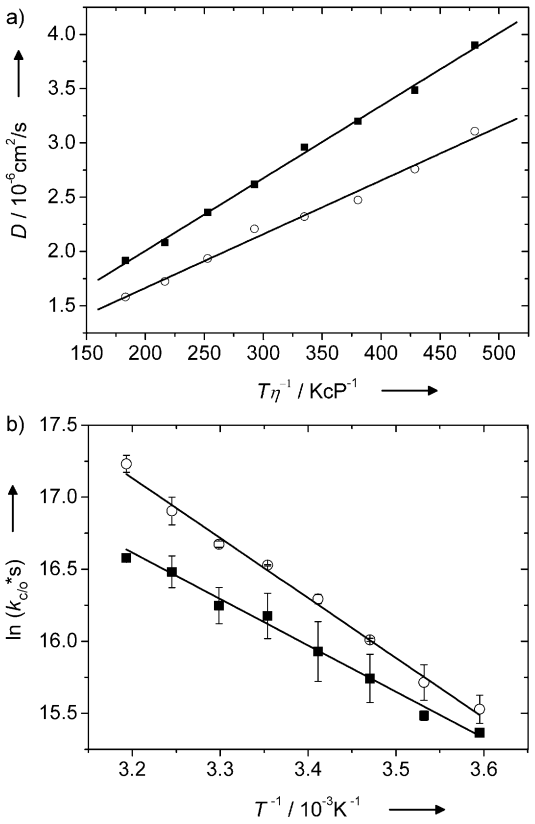

Figure 3. a) Translational diffusion constants are plotted as function of $T/\eta(T)$ according to the Stokes–Einstein relation [Eq. (S3), Supporting Information] for MR121-[Gly-Ser-]$_8$Trp (■) and MR121-[Ser(β-Gal)-Gly-]$_8$Trp (○). Straight lines represent the linear regression curve. b) Arrhenius plots of contact formation rate constants k_c (■) and opening rate constants k_o (○) for MR121-[Ser(β-Gal)-Gly-]$_8$Trp. The data is measured in aqueous solution and slopes reveal enthalpic activation barriers of (26 ± 1) kJ mol^{-1} and (36 ± 2) kJ mol^{-1}, respectively. Error bars represent standard deviations of two measurements.

Monitoring k_c and k_o as function of temperature (5–40 °C) by FCS revealed Arrhenius temperature dependence for both the closing and opening processes (Figure 3). The contact formation rate constants k_c for MR121-[Ser(β-Gal)-Gly-]$_8$Trp reveal an enthalpic activation barrier of 26 ± 1 kJ mol^{-1}, significantly larger than the mostly viscosity-related activation barrier of 18 ± 3 kJ mol^{-1} measured for poly-GS.[9d] A mere increase of ~8 kJ mol^{-1} in activation enthalpy would induce a ~26 fold decrease of contact formation rates at 20 °C. Since we observe changes in rate constants of a factor between 3 and 4 only, a variation in the temperature-independent preexponential factor, including all entropy changes must induce some compensation and reduce the overall activation barrier.

Activation enthalpies for the opening process amount to 36 ± 2 kJ mol^{-1} and are only slightly larger than those previously observed for MR121-[Gly-Ser-]$_x$Trp (on the order of 30 kJ mol^{-1}).[9d] In bimolecular interaction studies such opening enthalpies were found to reflect van der Waals interactions between fluorophore and Trp.[9b] It is likely that in the peptide similar interactions stabilize the closed stacked complex and need to be overcome before the polymer stretches out again.

In order to unravel how rates are reduced by glycosylation, we next studied the viscosity dependence of rate constants. After measuring end-to-end contact formation rate constants for MR121-[Ser(β-Gal)-Gly-]$_8$Trp in solutions with a sucrose concentration between 0% and 50% (w/v), we plotted the inverse rate constants as function of viscosity in the range of ~1 to ~15 cP and for 20 and 40 °C (Figure 4). At viscosities above approximately 5 cP, at which the main correlation decay approaches microsecond times scales, a second exponential component on time scales around 10 ns appeared albeit with smaller amplitudes. This fast decay component is independent of the quenching interactions and originates from rotational diffusion of the molecule. Whenever the fluorophore dipole is oriented parallel to the optical axis no excitation occurs and the fluorescence is effectively switched off.

The inverse contact formation and opening rate constants derived from the slower component follow a viscosity dependence that is linear up to approximately 5 cP. For higher viscosities a deviation towards higher rate constants (smaller time constants) was observed. The reason for this deviation from linearity, which is larger than previously observed for Gly-Ser peptides,[9d,12] is not known. Fitting the data between 0 and 5 cP with a linear function revealed a *y*-intercept (± standard error) for $\tau_c = 1/k_c$ ($\tau_o = 1/k_o$) of $(-3.6 \pm 1.2) \times 10^{-8}$ s [$(2.3 \pm 0.5) \times$

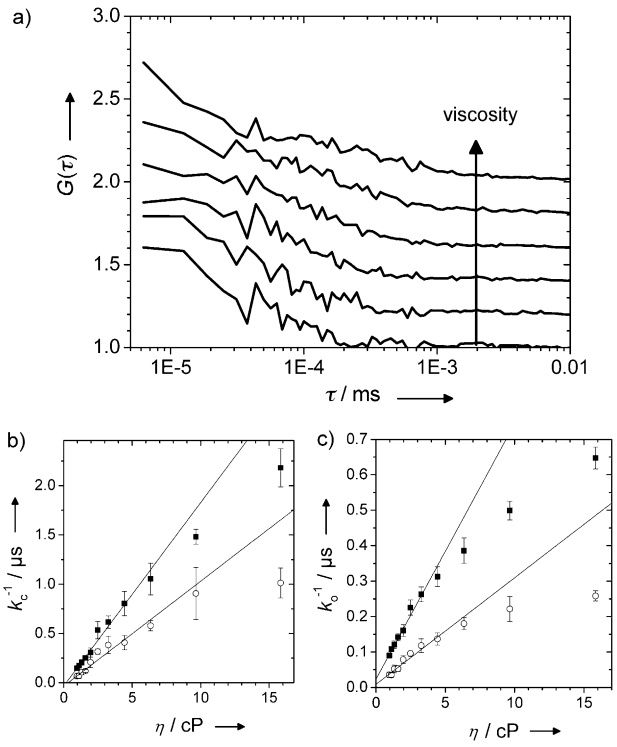

Figure 4. a) FCS data of MR121-[Ser(β-Gal)-Gly-]$_8$Trp recorded at various viscosities and shown for 20 °C. The inset shows the fast correlation decay on nanosecond time scales from which contact formation and opening rate constants (k_c and k_o, respectively) are derived. Data curves are offset by 0.2. At larger viscosities the decay is composed of two exponential components of which the slower component represents loop closure and the faster component rotational diffusion of the whole molecule. b), c) Inverse rate constants ($1/k_c$ in b and $1/k_o$ in c) are shown as derived from the slower decay component for various viscosities at 20 °C (■) and 40 °C (○).

10^{-8} s] at 20 °C and of $(-3.7 \pm 2.5) \times 10^{-8}$ s [$(0.8 \pm 0.6) \times 10^{-8}$ s] at 40 °C. The precise values depend on the upper limit for the fitting range and are for all four data curves consistent with a zero *y*-intercept. This observation resembles previous results for MR121-[Gly-Ser-]$_x$Trp[9d] and proves that no viscosity-independent energy-dissipating effects from intramolecular interactions resembling internal friction[13] slow down conformational dynamics. The data provides strong evidence that end-to-end contact formation rates of glycopeptides are fully controlled by the frictional drag between solvent and peptide.

Our data reveal that glycosylation reduces end-to-end contact formation rates partly by increasing the viscosity-independent contribution to the activation barrier. Formally this is expressed by an equation that consists of a viscosity-independent exponential term representing the activation enthalpy ΔH and a pre-exponential factor that is the product of a temperature-independent term and the inverse solvent viscosity: $k_c = C/\eta(T) \times \exp(\Delta H/k_b T)$. This relation is consistent with purely diffusive motion as described by Kramers's theory.[13,14]

Interactions between the fluorophore and attached sugar residues are negligible as was confirmed by time-resolved anisotropy measurements. We found identical rotation times of a few hundred picoseconds in non-glycosylated and glycosylated Ser-Gly peptides, indicating that the fluorophore revolves around its molecular linker with the same degrees of freedom in both peptides. Thus the additional interactions slowing down conformational dynamics and increasing the hydrodynamic radius must be due to glycans interacting with each other or with the peptide backbone.

Enthalpic contributions to the activation barrier might have its origin in the rotation of glycan chains together with dihedral angle rotation of the peptide backbone during conformational dynamics of the peptide. Entropic contributions might be introduced by steric constraints from the glycan chains attached to the peptide backbone. If attractive intramolecular hydrogen bonding between glycans or between glycan and backbone atoms slowed down conformational dynamics they would have had to be sufficiently strong in comparison to hydrogen bonding interactions between glycans and water or dissolved sucrose. Such interactions would then have had to resemble a contribution of intramolecular internal friction that would have been visible as viscosity-independent (offset) component in the viscosity plots (Figure 4), contrary to our observation.

According to theoretical treatments [for instance in the Svabo–Schulten–Schulten (SSS) theory[15]] contact formation rate constants depend on chain dynamics as expressed by an intramolecular diffusion constant and on the equilibrium distribution of end-to-end distances. Assuming that R_h is proportional to the root mean square end-to-end distance SSS theory predicts that rate constants scale with one over the third power of R_h. Our estimate of $R_h(-\text{Gal})/R_h(+\text{Gal}) = 0.74 \pm 0.03$ results in a change of rate constants by no more than 2.5 at 20 °C. This estimate confirms that the observed 3- to 4-fold slowdown is not only due to equilibrium properties but also influences the intramolecular diffusion constant.

It was previously suggested by computer simulations that glycosylation of a denatured protein increases both enthalpy and entropy of the unfolded state.[16] The increase in enthalpy was larger than the increase in entropy and this was interpreted as a hindrance of intramolecular interactions (or in other words as limiting residual structure formation) in the unfolded state due to the attached glycans and resulting in more extended conformations. Qualitatively we now observe a similar effect in fully unstructured peptides for the transition state ensemble. There is computational and experimental evidence that conformational dynamics of unstructured non-glycosylated peptides are mediated by transient hydrogen bonding between backbone atoms.[11,17] Our results might indicate that the bonding dynamics between peptide backbone atoms are modified by attached carbohydrates through shielding of backbone–backbone hydrogen bond interactions.

Overall we found that β-galactosyl residues attached across an *O*-glycosidic bond to serine residues in Ser-Gly peptides slow down intramolecular conformational dynamics. The change in dynamics is accompanied by an increase of the hydrodynamic radius consistent with observations for unfolded glycoproteins.[18] Arrhenius temperature dependence reveals increased activation enthalpies accompanied by a certain degree of enthalpy-entropy compensation. Rate constants at 20 and 40 °C were viscosity-controlled and did not show any signature of internal friction. The data suggests that attached glycans have a strong impact on the dynamic properties of unstructured and unfolded proteins.

Acknowledgements

We thank Prof. K. H. Drexhage for provision of MR121. The work was funded by the German Research Foundation (SFB 613) and the German Israel Foundation (Young Scientists Program).

Keywords: biophysics · fluorescence correlation spectroscopy · glycopeptides · glycosylation · protein dynamics

[1] H.-J. Gabius in *The Sugar Code. Fundamentals of glycosciences* (Ed.: H.-J. Gabius), Wiley-VCH, Weinheim, **2009**.
[2] H. Lis, N. Sharon, *Chem. Rev.* **1998**, *98*, 637–674.
[3] a) N. Mitra, S. Sinha, T. N. C. Ramya, A. Surolia, *Trends Biochem. Sci.* **2006**, *31*, 156–163; b) D. Shental-Bechor, Y. Levy, *Curr. Opin. Struct. Biol.* **2009**, *19*, 524–533; c) B. Imperiali, *Acc. Chem. Res.* **1997**, *30*, 452–459.
[4] Y. Tachibana, G. L. Fletcher, N. Fujitani, S. Tsuda, K. Monde, S. Nishimura, *Angew. Chem.* **2004**, *116*, 874–880; *Angew. Chem. Int. Ed.* **2004**, *43*, 856–862.
[5] M. R. Wormald, A. J. Petrescu, Y. L. Pao, A. Glithero, T. Elliott, R. A. Dwek, *Chem. Rev.* **2002**, *102*, 371–386.
[6] R. Bansil, E. Stanley, J. T. LaMont, *Annu. Rev. Physiol.* **1995**, *57*, 635–657.
[7] B. Imperiali, S. E. O'Connor, *Curr. Opin. Chem. Biol.* **1999**, *3*, 643–649.
[8] a) S. T. Hess, S. Huang, A. A. Heikal, W. W. Webb, *Biochemistry* **2002**, *41*, 697–705; b) D. Magde, E. L. Elson, W. W. Webb, *Biopolymers* **1974**, *13*, 29–61.
[9] a) S. Doose, H. Neuweiler, M. Sauer, *ChemPhysChem* **2009**, *10*, 1389–1398; b) S. Doose, H. Neuweiler, M. Sauer, *ChemPhysChem* **2005**, *6*, 2277–2285; c) H. Neuweiler, S. Doose, M. Sauer, *Proc. Natl. Acad. Sci. USA* **2005**, *102*, 16650–16655; d) H. Neuweiler, M. Löllmann, S. Doose, M. Sauer, *J. Mol. Biol.* **2007**, *365*, 856–869; e) S. Doose, H. Neuweiler, H. Barsch, M. Sauer, *Proc. Natl. Acad. Sci. USA* **2007**, *104*, 17400–17405;

f) H. Neuweiler, M. Sauer, *Curr. Pharm. Biotechnol.* **2004**, *5*, 285 – 298; g) J. Kim, S. Doose, H. Neuweiler, M. Sauer, *Nucleic Acids Res.* **2006**, *34*, 2516 – 2527.
[10] J. R. Lakowicz, *Principles of Fluorescence Spectroscopy, 2 ed.*, Plenum, New York, **1999**.
[11] I. Daidone, H. Neuweiler, S. Doose, M. Sauer, J. C. Smith, *PLoS Comput. Biol.* **2010**, *6*, e1000645.
[12] A. Möglich, F. Krieger, T. Kiefhaber, *J. Mol. Biol.* **2005**, *345*, 153 – 162.
[13] S. J. Hagen, *Curr. Protein Pept. Sci.* **2010**, *11*, 385 – 395.
[14] H. A. Kramers, *Physica* **1940**, *7*, 284 – 304.
[15] A. Szabo, K. Schulten, Z. Schulten, *J. Chem. Phys.* **1980**, *72*, 4350 – 4357.
[16] D. Shental-Bechor, Y. Levy, *Proc. Natl. Acad. Sci. USA* **2008**, *105*, 8256 – 8261.
[17] a) D. P. Teufel, C. M. Johnson, J. K. Lum, H. Neuweiler, *J. Mol. Biol.* **2011**, *409*, 250 – 262; b) A. Möglich, K. Joder, T. Kiefhaber, *Proc. Natl. Acad. Sci. USA* **2006**, *103*, 12 394 – 12 399.
[18] a) R. Hoiberg-Nielsen, P. Westh, L. Arleth, *Biophys. J.* **2009**, *96*, 153 – 161; b) R. Shogren, T. A. Gerken, N. Jentoft, *Biochemistry* **1989**, *28*, 5525 – 5536.
[19] M. Mathlouthi, J. Génotelle in *Sucrose, Properties and Applications* (Eds.: M. Mathlouthi, P. Reiser), Blackie Academic & Professional, London, **1995**, pp. 126 – 154.

Received: August 23, 2011
Published online on September 16, 2011

